DOI 10.1007/s10891-018-1787-y

*Journal of Engineering Physics and Thermophysics,* Vol. 91, No. 3, May, 2018

# FEATURES OF HIGH-VELOCITY PENETRATION AND MOTION OF SUPERCAVITATING KINETIC STRIKERS IN WATER

**V. V. Burkin, R. N. Akinshin, S. A. Afanas′eva, I. L. Borisenkov, A. N. Ishchenko, M. V. Khabibullin, A. V. Chupashev, and N. T. Yugov**

UDC 539.3; 623.562.6

*Consideration is given to conditions ensuring stable high-velocity motion of supercavitating kinetic strikers in water. To investigate the stressed-strained state and a possible destruction of solid bodies during the motion in water and in interaction with underwater barriers of various types, the authors carry out mathematical modeling based on a unified methodological approach of the continuum mechanics. The range of the velocities under study is 500–1590 m/s. Results of the group start of supercavitating strikers are given.*

***Keywords:*** *water, supercavitating kinetic strikers, barrier, high-velocity penetration, stability of motion, experimental mathematical modeling.*

**Introduction.** Investigation of the high-speed interaction of bodies in water is aimed at solving a number of interconnected problems: imparting a high initial velocity, overcoming the resistance of water, and ensuring stable motion and efficient interaction with underwater barriers. At present, there is a great body of data in the literature on each problem of this set. To reduce the resistance of a body during its motion in water, use is made of the phenomenon of cavitation: the formation of a gas-filled cavity in water, which envelopes the underwater striker [1, 2]. High-velocity motion of metallic strikers of conical shape in water has been the focus of a theoretical and experimental analysis [3–5]. Visualization of fast processes occupies a special place, in particular, optical methods of diagnostics have been developed [6, 7]. The procedure of investigation of the high-speed interaction of the striker from hardmetal materials and water [8, 9] makes it possible to determine the instant and character of its destruction.

In the case of the high-velocity entry into water and of motion in it, there arise problems connected with the dynamics of motion of the body in water, the interaction with nonstationary free boundaries under supercavitation conditions, etc. Overcoming the water resistance during the high-velocity motion of the body is a governing factor both in the initial stage of penetration into the water and at a depth, whose influence should be minimized. Depending on velocity, different conditions can be implemented for the interaction between the body and the aqueous medium: subsonic, transonic, and supersonic ones, which are accompanied by the characteristic physical phenomena affecting the resistance to motion. In the range in question, there are different reactions of the material of the striker to loading in its interaction with water: from minor plastic strains to destruction. The state of the striker when it enters the water is the key factor for ensuring its stable motion on the water track.

The present work seeks to develop a set of experimental procedures and theoretical methods and to study, from them, major factors of high-velocity motion of thin conical bodies in water. On the basis of the developed experimental and theoretical hydroballistics complex [10, 11], one can investigate high-velocity motion of supercavitating kinetic strikers in water in a wide range of velocities, and also their interaction with underwater barriers, including the case of group gun start. Particular emphasis is placed on visualization of fast processes. To investigate the stressed-strained state and a possible destruction of solid bodies during the motion in water and in interaction with underwater barriers of various types, we use mathematical models based on a unified methodological approach of continuum mechanics [12]. These models were implemented in software systems in a two-dimensional formulation by a modified large-particle method [13] and in a complete three-dimensional formulation by a modified finite-element method [14].

**Design and Experimental Analysis.** The laboratory hydroballistics bench (Fig. 1) is a closed ballistic track. The projectile assembly including the striker under study and the driver is accelerated in the barrel of a ballistic installation (I)

National Research Tomsk State University, 36 Lenin Ave., Tomsk, 634050, Russia; email: s.a.afanasyeva@mail.ru.
Translated from Inzhenerno-Fizicheskii Zhurnal, Vol. 91, No. 3, pp. 701–708, May–June, 2018. Original article submitted July 1, 2017.

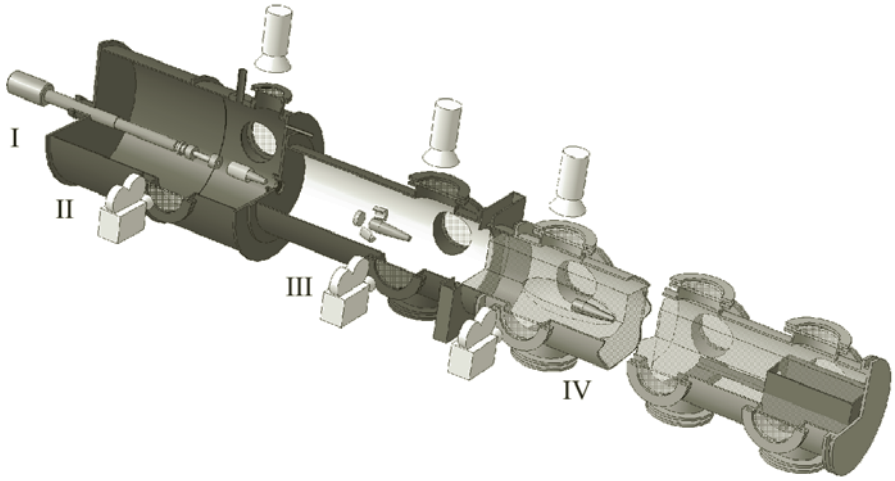


Fig. 1. Hydroballistics bench: I, powder ballistic installation; II, evaluated part of the track; III, aerodynamic part of the track; hydrodynamic part of the track; IV, targetry.

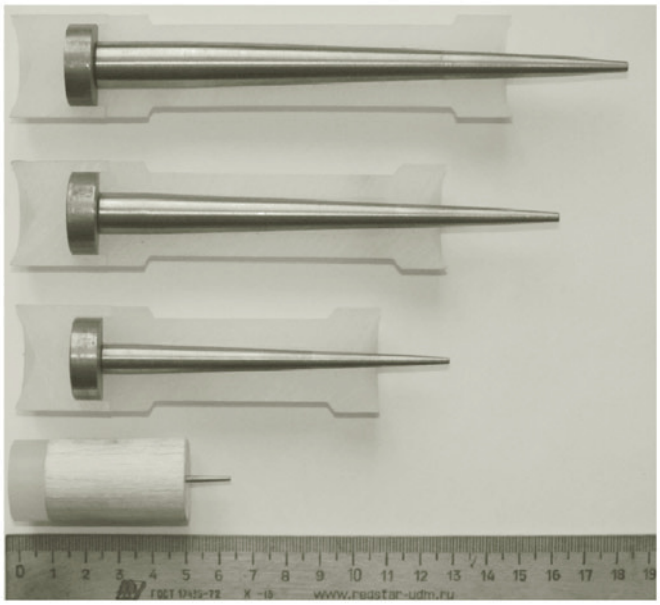

Fig. 2. External view of typical supercavitating kinetic strikers in drivers.

to a required velocity which is ensured by the selection of a powder-charge sample. The evacuated part of the track (II) is necessary as the suppressor; there, hot explosive gases cool down. In the aerodynamic part of the track (III), we have the separation of the driver from the striker. Next, the striker enters the hydrodynamic part of the track (IV) whose length is 10 m; there, the targetry is located.

The velocity of motion of the striker is recorded in the barrel using a Doppler velocity meter in the DDS-6000 barrel [15], at exit from the barrel using a muzzle velocity sensor (MVS) [16], and on the path before its contact with the target. In any part of the track, once the striker leaves the barrel, we can visually record, via special ports, the state of the body and its location throughout the path until it reaches the targetry. On employment of different video and photorecording methods, a considerable volume of information is stored and processed on a measuring and recording system. Video cameras are installed in the evaluated, aerodynamic, and hydrodynamic parts of the track. Direct observation of the motion of bodies using the Phantom v177 and Cordin 530 high-speed video cameras on the aerodynamic portion of the track enables us to

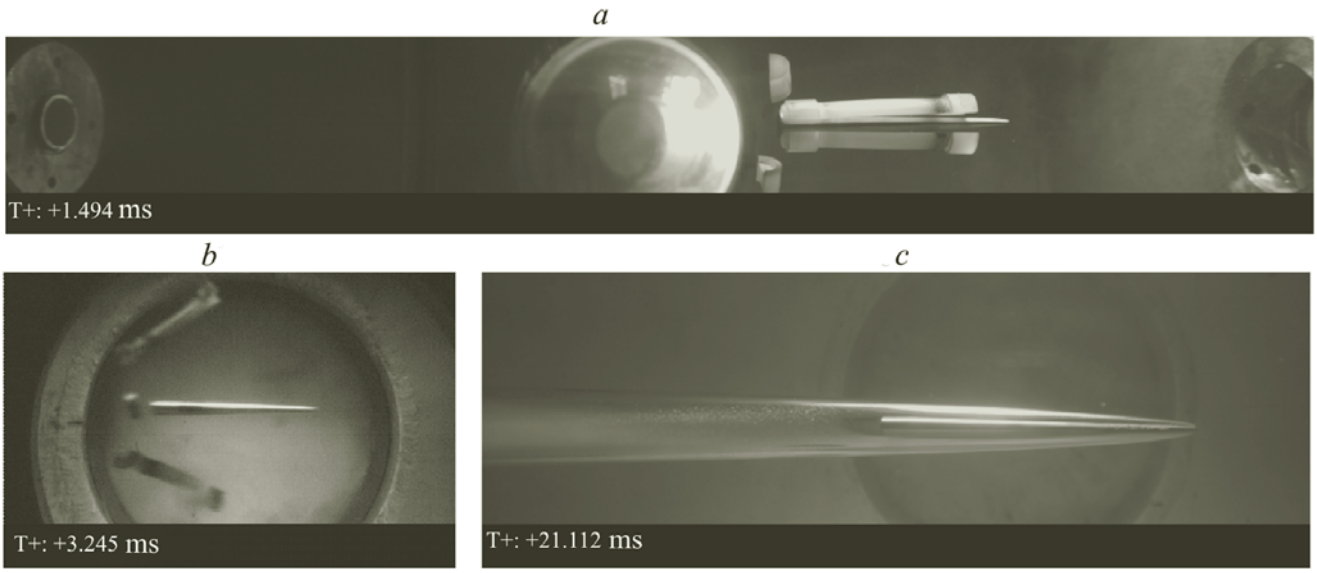


Fig. 3. Photographic record of motion of a supercavitating kinetic striker in the initial stage: a) in the evacuated, b) aerodynamic, and c) hydrodynamic part of the track.

select optimum structures for the drivers fabricated from various materials such as textolite, polyethylene, cork, and balsa wood, ensuring timely separation from the striker with a minimum perturbation. Studying the behavior of the bodies in the hydrodynamic part of the path makes it possible to assess the body′s state externally, to record the characteristics of motion, and to correct, from these data, its shape or select a structural material so as to ensure the strength and stable motion on the track.

The given hydroballistics complex is used for studying the motion of supercavitating kinetic strikers in water in a wide velocity range. Figure 2 gives typical conical supercavitating kinetic strikers with an end cavitator of varying diameter $d_0$, fabricated from steel and high-strength tungsten + nickel + iron (W–Ni–Fe) alloy and placed in the drivers.

A compulsory condition for the stable motion of a supercavitating kinetic striker in water is the separation of the driver on the air portion of the path. Nonetheless, on entry into the water, there can be a slight deviation of the axis of the supercavitating kinetic striker from the velocity vector, which must be compensated for on the initial portion of the path. The process of stabilization of the supercavitating kinetic striker in water is not instantaneous. High pressures on the surface of contact between the cavitator and the water keep the cavitator from leaving the path. The supercavitating kinetic striker glides inside the cavity for some time.

Figure 3 gives the motion of the supercavitating kinetic striker of mass $m$ = 58 g with a separated driver after leaving the bore of the ballistic installation with velocity $V_m$ = 970 m/s in the initial stage of motion. In the track′s evacuated part, the aftereffect of explosive gases results in the separation of a push tray, and the stage of opening of the driver begins (Fig. 3a). Figure 3b gives the motion of the projectile assembly on the air portion of the track after covering a distance of 2.0 m. Full separation of the driver from the supercavitating kinetic striker moving without deviations from the axis of the path up to the entry into the track′s hydrodynamic part is observed (Fig. 3c). The high-pressure region in the zone adjacent to the forebody, which moves together with the supercavitating kinetic striker, may lead to plastic strain of the cavitator and even its destruction. Figure 4 shows the end and profile of the cavitator of the supercavitating kinetic striker fabricated from steel [3] (a) at the velocity of entry into the water $V_0$ = 1090 m/s and from W–Ni–Fe (b) at $V_0$ = 1553 m/s. The steel cavitator has undergone minor plastic strains (the ratio of the initial diameter to the final one is $d_0/d_f$ = 0.99); in the second case, at $d_0/d_f$ = 0.95, there is the initial stage of brittle fracture.

The microphotograph (Fig. 5) of the sections of the forebody of the W–Ni–Fe striker before (a) and after penetrating into the water (b) shows the presence of structural changes in the alloy (large conglomerates, tungsten, light interlayers, nickel, and iron). Increase in the velocity above the indicated values requires that the strength characteristics of materials used for fabricating supercavitating kinetic strikers be substantially improved.

The conditions of entry into the water and the size of the cavity of a supercavitating kinetic striker are substantially dependent on the cavitator diameter. To determine the characteristics of penetration of supercavitating kinetic strikers with

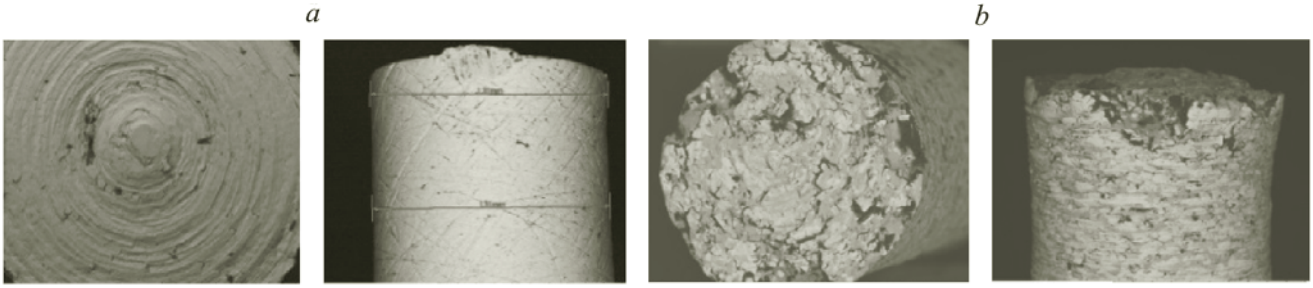


Fig. 4. Microphotographs of the end and lateral surfaces of the cavitators after the penetration of the strikers into the water: a) striker from steel and b) striker from W–Ni–Fe.

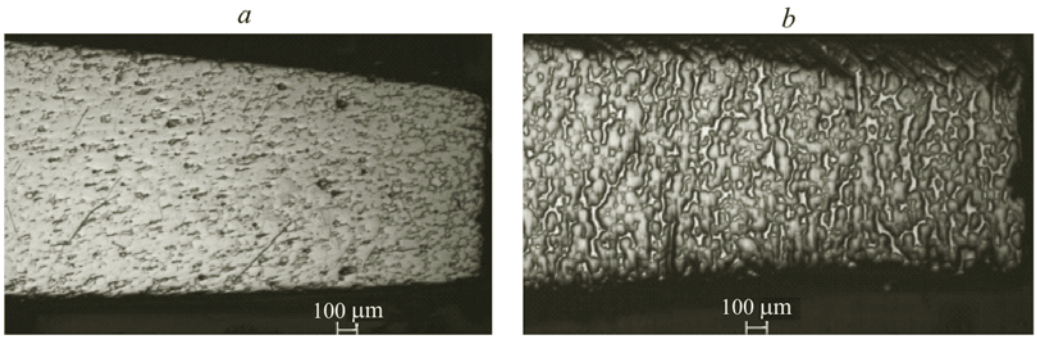


Fig. 5. Microphotograph of the section of the W–Ni–Fe cavitator: a) initial state of the material; b) state of the material on penetration into the water.

a varying cavitator diameter, we carried out mathematical modeling. Figure 6 gives results of calculation in a cylindrical coordinate system $r$, $z$: in the left half-plane, in the form of the distribution of the vector of the mass velocity $u$ with respect to the maximum value $U_{max}$, and in the right half-plane, in the form of the pressure distribution in the flow field (the pressure scale is in GPa). Also, the figure gives the values of the maximum pressure $P_{max}$ and of the center-of-mass velocity of the striker $V_{cm}$. The velocity of entry into the water is equal to $V_0$ = 824 m/s. The calculation was done to the instant of time $t$ at which the process of formation of a cavity of diameter $D$ in the afterbody of the striker is completed. When the supercavitating kinetic striker with an end cavitator of diameter $d_0$ = 1 mm penetrates, no supercavity is formed (Fig. 6a). Here, the striker is in contact with the cavity and is additionally decelerated. The supercavitating kinetic striker with a cavitator of diameter $d_0$ = 2 mm forms a supercavity of diameter $D$ = 26.2 mm (Fig. 6b). At $d_0$ = 3 mm, the supercavity diameter is equal to $D$ = 28.4 mm (Fig. 6c). The drop in the velocity illustrated in Fig. 7 demonstrates its dependence on the cavitator diameter.

Entry into the water in the presence of the angle of attack α (angle between the axis of the supercavitating kinetic striker and the velocity vector) may lead to additional dynamic loads on the supercavitating kinetic striker. Figure 8 gives the chronogram of the process of penetration of the supercavitating kinetic striker fabricated from W–Ni–Fe ($d_0$ = 2.3 mm and $m$ = 54.18 g) into the water at the angle of attack $\alpha = 3^o$. Only the forebody of the striker is strained, which does not affect the stable character of its subsequent penetration. As the angle of attack increases to $\alpha = 10^o$, there appear strong flexural strain and partial destruction of the forebody, which may give rise to a full stability loss during further motion.

The absence of the angle of attack at entry into the water ensures stable motion. Using, as an example, a W–Ni–Fe supercavitating kinetic striker ($d_0$ = 3.8 mm and $m$ = 163 g) which has entered the water with velocity $V_0$ = 594/8 m/s, we observe the stabilization of stable motion through the gliding when the supercavitating kinetic striker traverses a portion of 3.4 to 8.0 m in water. In the initial stage of gliding (Fig. 9a), the diameter of the cavity in the striker′s afterbody is $D$ = 32.9 mm, with the velocity of motion being 558.5 m/s. In the final stage of gliding, the diameter is $D$ = 31.2 mm and the velocity is 502.9 m/s (Fig. 9b). After covering 4.6 m in water, the supercavitating kinetic striker reaches the regime of stable motion. The gliding time on this portion is 9.437 ms. After covering the distance $L$ = 9.3 m in water, the supercavitating kinetic striker

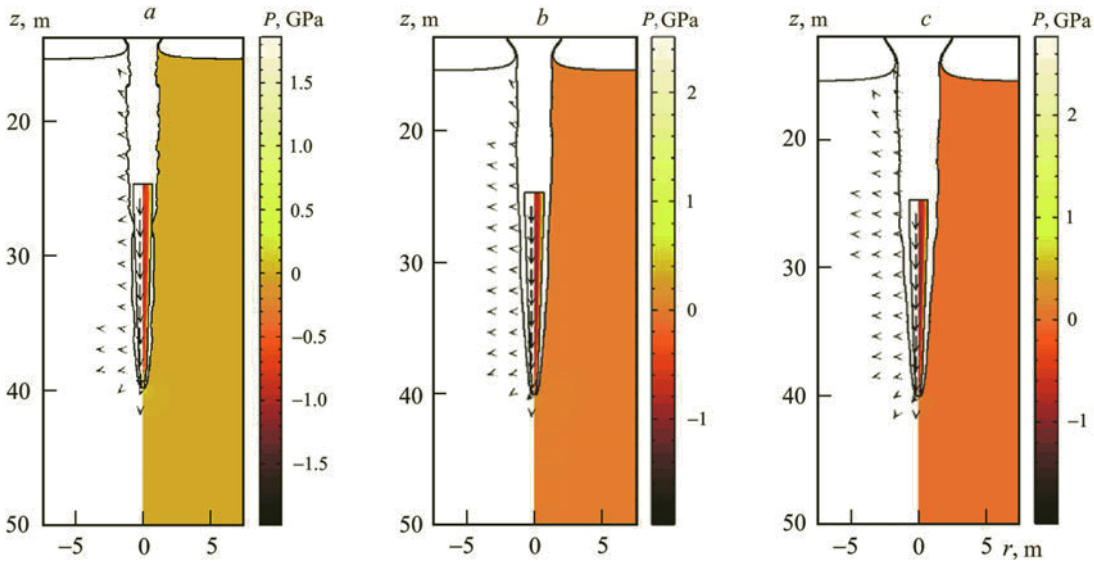


Fig. 6. Formation of the supercavity: a) $d_0 = 1$ mm, $t = 300$ μs, $D = 23$ mm, $P_{max} = 2.12$ GPa, $U_{max} = 841$ m/s, and $U_{cm} = 817$ m/s; b) $d_0 = 2$ mm, $t = 500$ μs, $D = 26.2$ mm, $P_{max} = 2.51$ GPa, $U_{max} = 850$ m/s, and $U_{cm} = 818$ m/s; c) $d_0 = 3$ mm, $t = 500$ μs, $D = 28.4$ mm, $P_{max} = 2.77$ GPa, $U_{max} = 848$ m/s, and $U_{cm} = 816$ m/s.

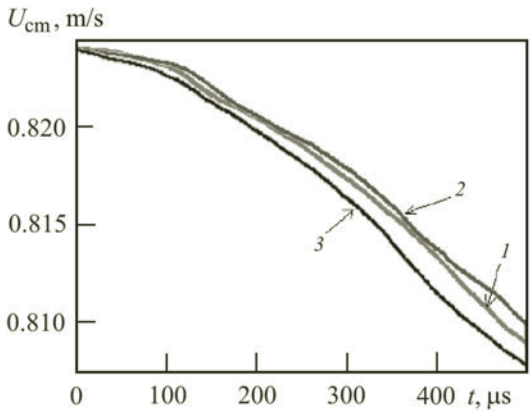


Fig. 7. Drop in the velocity of supercavitating kinetic strikers at different cavitator diameters: 1) $d_0 = 1$, 2) 2, and 3) 3 mm.

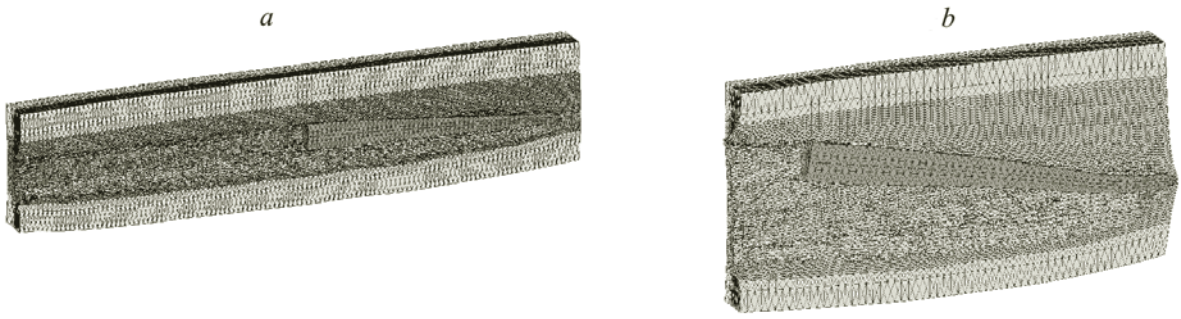


Fig. 8. Penetration of a supercavitating kinetic striker into the water at different angles of attack: a) $V_0 = 1098$ m/s, $\alpha = 3^o$, and $t = 188$ μs; b) $V_0 = 1262$ m/s, $\alpha = 10^o$, and $t = 92$ μs.

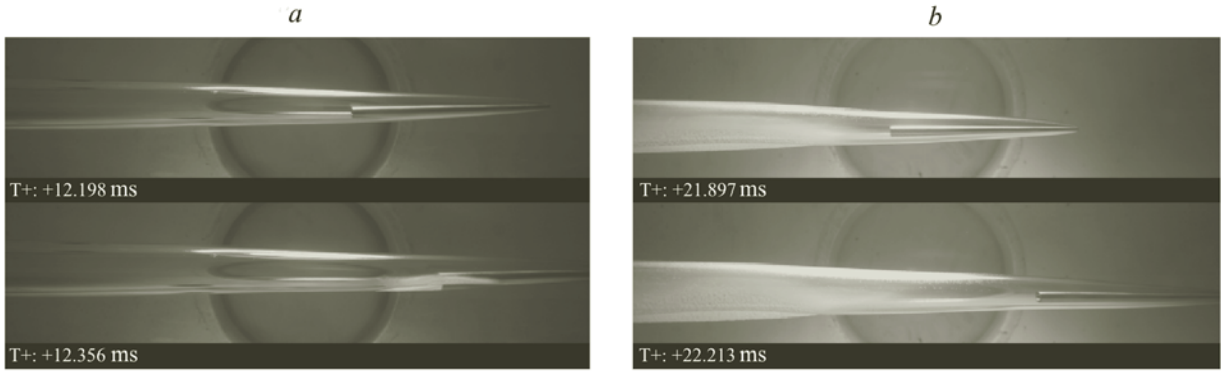


Fig. 9. Gliding of a supercavitating kinetic striker: a) initial stage at $t$ = 12.198–12.396 ms; b) final stage at $t$ = 21.897–22.213 ms.

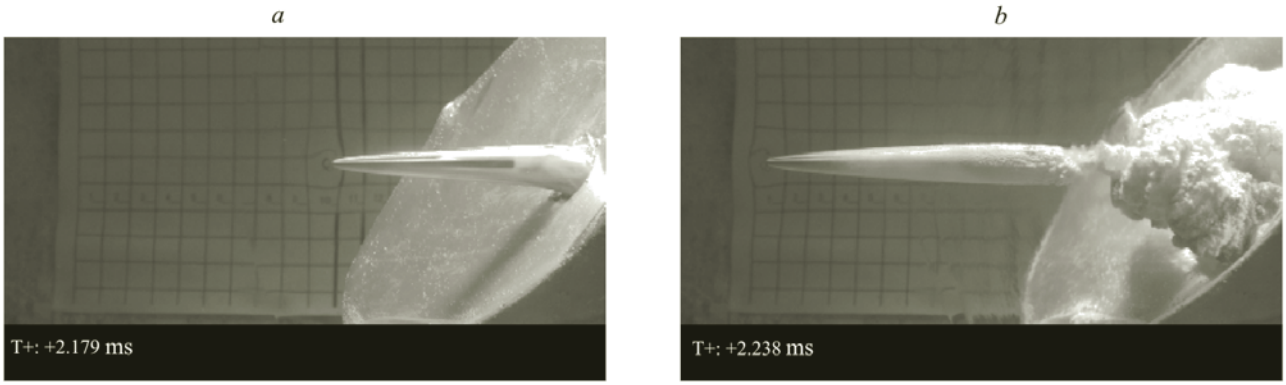


Fig. 10. Photographic record of the entry of a supercavitating kinetic striker into the water at the angle $\varphi = 45^{o}$: a) $t$ = 2.179 and b) 2.238 ms.

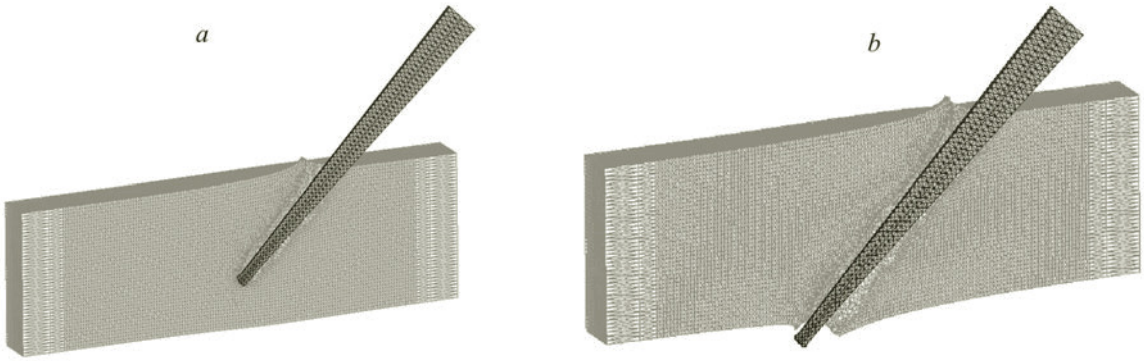


Fig. 11. Chronogram of the entry of a supercavitating kinetic striker into the water at $V_0$ = 1100 m/s and $\varphi = 45^{o}$: a) $t$ = 20 and b) 32 μs.

pierces a steel barrier of thickness 8 mm at the velocity $V \sim 490$ m/s with deviation from the aimpoint $D$ = 0.5 cm. The solid angle in which the deviation of the path of the supercavitating kinetic striker occurs does not exceed $0.03^{o}$.

The supercavitating kinetic striker fabricated from W–Ni–Fe alloy ($d_0$ = 1.23 mm and $m$ = 6.42 g) at the velocity $V_0$ = 1100 m/s exhibits stable motion at entry into the water at the angle $\alpha = 45^{o}$ (angle between the axis of the supercavitating kinetic striker and the normal to the water surface) (Fig. 10). Figure 11 gives results of mathematical modeling with conditions

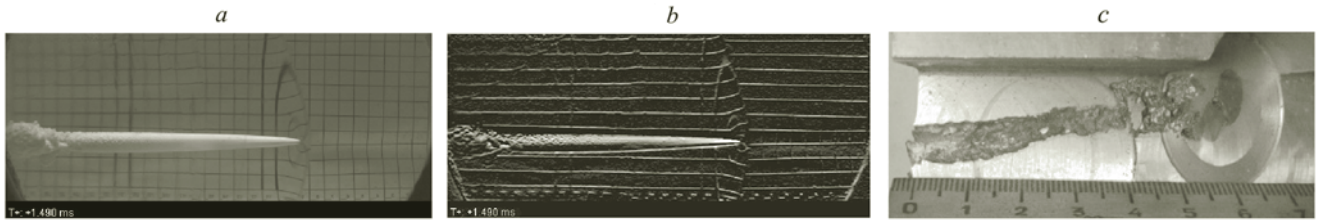


Fig. 12. Recording of the motion of a supercavitating kinetic striker in water and its interaction with the barrier at the velocity $U$ = 1590 m/s: a) initial image; b) image by the Sobell method; c) cut of the plate on collision.

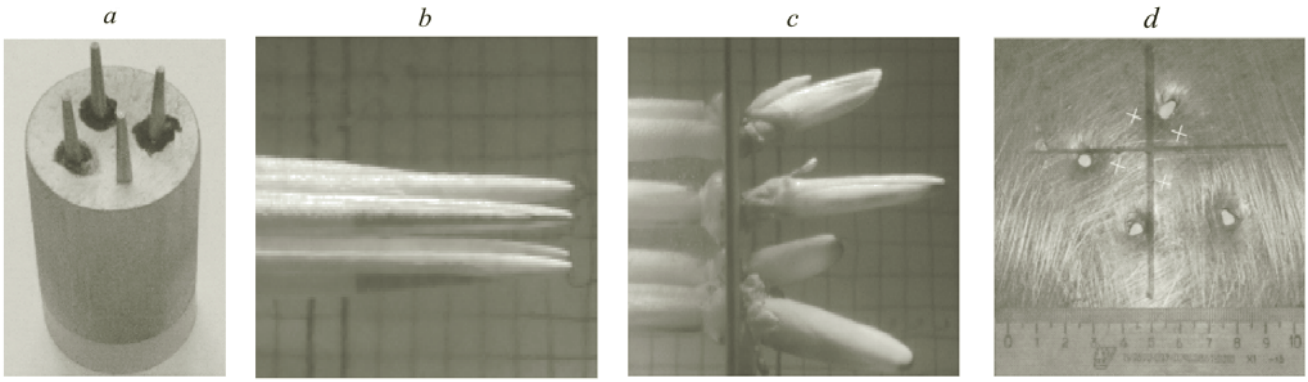


Fig. 13. Group motion of supercavitating kinetic strikers in water and the interaction with the underwater barrier: a) projectile assembly; b) motion on the hydroballistic track; c) interaction with the underwater barrier; d) view of the barrier on collision.

replicating the given experiment. The calculation was done to 32 μs. The striker velocity at this instant of time is 1091 m/s as in the experiment. The supercavitating kinetic striker has entered the water stably; no strain is observed in the forebody.

In the experiment presented in Fig. 12, the regime of supersonic motion of a W–Ni–Fe supercavitating kinetic striker of mass 5.76 g in water has been implemented. The supercavitating kinetic striker was accelerated in a ballistic installation of caliber 23 mm to the velocity $V_m$ = 1602 m/s. Stable motion of the projectile in water is observed. An attached shock wave is pronounced in the figure. In the water, at the distance $L$ = 1.26 mm, the supercavitating kinetic striker interacts with the Duralumin barrier of thickness 103 mm, forming a crater of depth 62 mm.

Figure 13 gives results of group throwing of four steel supercavitating kinetic strikers (at $d_0$ = 1.2 mm and $m$ = 2.7 g each) with muzzle velocity $V_m$ = 906 m/s and their interaction with the barrier of thickness 1 mm to be found in water at the distance $L$ = 1 m. The supercavitating kinetic strikers move synchronously in water and interact with the underwater barrier. Their movement relative to each other within the solid angle is noticed. From the position of the holes from the strikers on the target, the maximum solid angle, in which the group of supercavitating kinetic strikers is moving, is $1.5^o$. On interaction with the barrier, the angle of scattering of the strikers increases.

**Conclusions.** We made the design and experimental analysis of different steps of motion of a supercavitating kinetic striker in water, which has enabled us to find the regimes of stable motion of the supercavitating kinetic striker in water. The high throwing velocities reached impose stringent requirements on the strength of the supercavitating kinetic striker.

The developed procedure of investigation of the high-velocity penetration of supercavitating kinetic strikers into water makes it possible to study subsonic, trans-, and supersonic motions of supercavitating kinetic strikers in water, including the case of group gun start.

**Acknowledgment.** In the article, we have used the results obtained during the implementation of project No. 9.9036.2017/8.9 within the framework of the State Assignment of the Ministry of Education and Science of the Russian Federation.

## NOTATION

$D$, diameter of the cavity at the base of the cone of the striker, mm; $d_0$, initial diameter of the striker′s cavitator, mm; $d_c$, diameter of the striker′s cavitator after the experiment, mm; $L$, distance in water, m; $m$, mass of the supercavitating kinetic striker, g; $P_{max}$, maximum pressure, GPa; $r$, cylindrical coordinates, cm; $t$, time, μs; $V$, average velocity of the supercavitating kinetic striker on the observed portion, m/s; $V_m$, muzzle velocity of the projectile assembly, m/s; $V_0$, velocity of the supercavitating kinetic striker at entry into the water, m/s; $U_{cm}$, center-of-mass velocity of the supercavitating kinetic striker, m/s; α, angle of attack, deg; φ, angle of entry into the water, deg; Δ, deviation from the aimpoint, cm.

## REFERENCES


1. Marshall P. Tulin, Fifty years of supercavitating flow research in the United States: Personal Recollections, *Prikl. Gidromekh*., **2 (74)**, No. 3, 100–107 (2000).
2. Yu. N. Savchenko and A. N. Zverkhovskii, Procedure for conducting experiments on high-velocity motion of inertial models in water in a supercavitation regime, *Prikl. Gidromekh*., **11**, No. 4, 69–75 (2009).
3. A. N. Ishchenko, S. A. Afanas′eva, V. V. Burkin, et al., Theoretical and experimental analysis of the high-velocity interaction of solid bodies in water, *J. Eng. Phys. Thermophys*., **87**, No. 2, 399–408 (2014).
4. A. N. Ishchenko, R. N. Akinshin, S. A. Afanas′eva, et al., High-velocity motion of supercavitating bodies in water and their interaction with underwater barriers, *Fundam. Prikl. Gidrofiz*., **8**, No. 4, 5–10 (2015).
5. A. N. Ishchenko, S. A. Afanas′eva, N. N. Belov, et al., Experimental and mathematical modeling of high-velocity collision of a conical striker with various barriers, *J. Eng. Phys. Thermophys*., **90**, No. 4, 1018–1024 (2017).
6. N. Fomin, W. Merzkirch, D. Vitkin, and H. Wintrich, Visualization of turbulence anisotropy by single exposure speckle photography, *Exp. Fluids*, **20**, 476–479 (1996).
7. D. Vitkin, W. Merzkirch, and N. Fomin, Quantitative visualization of the change of turbulence structure caused by a normal shock wave, *J. Vis.*, **1**, No. 1, 29–35 (1998).
8. G. B. Chernyak and K. B. Povarova, *Tungsten in Service Ammunition* [in Russian], GNTs RF FGUP "TsNIIKhM," Moscow (2014).
9. O. Anderson, P. Lundberg, A. Helte, and P. Magnusson, Critical impact velocity of a cemented carbide projectile penetration a water target, *Proc. 26th Int. Symp. on Ballistics*, Miami, Fl (2011), pp. 1709–1718.
10. V. A. Burakov, V. V. Burkin, A. N. Ishchenko, et al., *Experimental Ballistics Complex*, Pending Patent Application No. 2015113676 of 13.04.2015. Federal Service for Intellectual Property, Patents, and Trademarks.
11. A. N. Ishchenko, R. N. Akinshin, S. A. Afanas′eva, et al., *Hydroballistics Complex for Investigation of the Capabilities of Underwater Kinetic Weapon. Fundamental Science — To the Navy.* Vol. 2. Proc. Roundtable Discussion within the framework of the VII Navy Salon, Tekhnosfera, Moscow (2016), pp. 214–232.
12. L. I. Sedov, *Mechanics of a Continuous Medium* [in Russian], Vols. 1 and 2, Nauka, Moscow (1973).
13. M. V. Khabibullin and S. A. Afanas′eva, *Calculation of Phenomena Occurring in Condensed Media as a Result of the Action on Them of Intense Pulses in the Axisymmetric Formulation*, Federal Service for Intellectual Property, Patents, and Trademarks, Certificate Acknowledging Registration of Computer Program No. 2012617301, Moscow, 14.08.2012.
14. N. T. Yugov, N. N. Belov, and A. A. Yugov, *Calculation of Adiabatic Nonstandard Flows in a Three-Dimensional Formulation (RANET-3). Package of Computer Programs*. Federal Service for Intellectual Property, Patents, and Trademarks. Certificate of State Registration of Computer Programs No. 2010611042, Moscow (2010).
15. *Meter of Velocity in the DDS-6000 Barrel: A Passport* [in Russian], Tais, Moscow (2010).
16. V. V. Burkin, A. A. D′yachkovskii, A. L. Egorov, et al., *Muzzle Velocity Sensor*, Patent No. 161396. Application RU 2015127042, Moscow, 06.07.2015. Federal Service for Intellectual Property, Patents, and Trademarks.